Available online at www.sciencedirect.com
SCIENCE DIRECT®
ELSEVIER
Earth and Planetary Science Letters 216 (2003) 43–54
EPSL
www.elsevier.com/locate/epsl

The formation of shatter cones by shock wave interference during impacting

D. Baratoux [a,*], H.J. Melosh [b]

[a] *Laboratoire Dynamique Terrestre et Planétaire, 14, Avenue Edouard Belin, 31000 Toulouse, France*
[b] *Lunar and Planetary Laboratory, University of Arizona, Tucson, AZ 85721, USA*

Received 1 April 2003; received in revised form 22 July 2003; accepted 20 August 2003

Abstract

In this paper we present a new model for the formation of shatter cones. The model follows earlier suggestions that shatter cones are initiated by heterogeneities in the rock, but does not require the participation of an elastic precursor wave: the conical fractures are initiated after the passage of the main plastic compression pulse, not before. Numerical simulations using the hydrocode SALE 2D, enhanced by the Grady–Kipp–Melosh fragmentation model, support the model. The conditions required for the formation of shatter cones are explored numerically and are found to be consistent with the pressure range derived from both explosion experiments and the analysis of shock metamorphic features in impact structures. This model permits us to deduce quantitative information about the shape of the shock wave from the shape and size of the observed shatter cones. Indeed, the occurrence of shatter cones is correlated with the ratio between the width of the compressive pulse and the size of the heterogeneity that initiates the conical fracture. The apical angles of the shatter cones are controlled by the shape of the rarefaction wave.

Keywords: shatter cones; impact craters; shock waves

1. Introduction

Shatter cones are the characteristic form of rock fractures in impact structures. They have been used for decades as unequivocal fingerprints of meteoritic impacts on Earth [1]. The abundant data about shapes, apical angles, sizes and distribution of shatter cones for many terrestrial impact structures may provide insight into the determination of impact conditions and characteristics of shock waves produced by high-velocity projectiles in rocks. However, the conical shape of these fractures remains enigmatic to date, and a quantitative interpretation of the geometric parameters of these objects is therefore not possible.

Relevant models for the formation of shatter cones must be consistent with the following constraints given by the observations of shatter cones in various high-pressure shocked materials including natural impact structures and explosion experiments. Shatter cones are found over a broad range of sizes of impact structures. They have been reported beneath the floors of small craters

* Corresponding author. Tel.: +33-5-61-33-29-79.
E-mail addresses: david.baratoux@cnes.fr (D. Baratoux), jmelosh@lpl.arizona.edu (H.J. Melosh).

0012-821X/03/$ – see front matter © 2003 Elsevier B.V. All rights reserved.
doi:10.1016/S0012-821X(03)00474-6

such as Kaalijarvi, Estonia (110 m), Lonar, India (1800 m) and Ries, Germany (24 km) [2]. At Charlevoix, shatter cones are well developed about 7 km from the center of the crater, with a progressive decrease in quantity inward and outward [2]. The pressures reached during shatter cone formation can be estimated from shock metamorphic features [3]. Shock metamorphic minerals formed by high-pressure shocks (coesite, stishovite, shock-formed glass, planar features) are observed closer to the shock wave source, whereas shatter cones are commonly located further out from the shock source area. All these observations imply a restricted range of pressure allowing the formation of shatter cones. The minimum formation pressure appears to be 1 GPa [2], while the maximum pressure is usually a few GPa. However, at the Charlevoix structure shatter cones are found at pressures up to about 20 GPa. Shatter cones have also been produced by explosions in various rocks [2,4]. In these experiments shatter cones are also observed within a restricted pressure range that extends from 2 to 6 GPa [2].

The axes of shatter cones are generally described as pointing toward the shock wave source area in both natural impact structures and explosion experiments [1]. However, many cases of non-radial orientation are now known [5]. The size of natural shatter cones ranges from a few centimeters to 12 m. Parts of cones or topless cones are more common than a complete conical surface and striations are observed at the surface of fractures while many features have also been interpreted as planar rather than conical [5–7]. Shatter cones can be organized in hierarchical structures often called horse-tail structures [7]. Apical angles are reported to vary from approximately 60 to 120° with an average value close to 90° [1,2,6,8]. The presence of spherules, indicating shock-induced melting, is reported at the Vredefort structure, South Africa [9,10].

The most widely accepted mechanism for the formation of shatter cones is based on a theoretical study of the phenomenon by Johnson and Talbot [11]. They proposed that shatter cones form when the elastic precursor of the shock front is scattered by a heterogeneity in the rock. Recently, Sagy et al. [7] restarted the debate about the formation of shatter cones and proposed a model to explain the formation of striations [7] and emphasized that numerous shatter cones are often planar rather than conical.

2. Mechanism for the formation of shatter cones

We propose that a particular tensional stress pattern, occurring in the presence of heterogeneities in the rock, is responsible for the formation of shatter cones. Our model relies on the interference of a scattered elastic wave by heterogeneities with the main stress wave in spherical geometry. This situation leads to a local increase in tensional stress producing curved fractures along conical surfaces. A clear understanding of the stress patterns that develop during the expansion of a spherical stress wave is a basic prerequisite to any model of shatter cone formation. Furthermore, because we propose that shatter cones are tensional fractures, it is important to understand when and where tensional stresses develop during the propagation of a shock wave. Before presenting our new model, we thus describe in detail the stresses in an expanding spherical shock wave.

2.1. Shock waves in spherical geometry

Although analytical solutions exist for the propagation of pure elastic waves in spherical geometry, there is no such solution for plastic or shock waves. To evaluate the radial and hoop stresses both at and behind the shock front, we performed a simple one-dimensional simulation in

Table 1
Material properties in the one-dimensional simulation of the propagation of a spherical shock wave

Density (kg/m^3)	Bulk modulus (GPa)	Shear modulus (GPa)	Murnhagan exponent	Hugoniot elastic limit (GPa)
3000	50	30	4	1

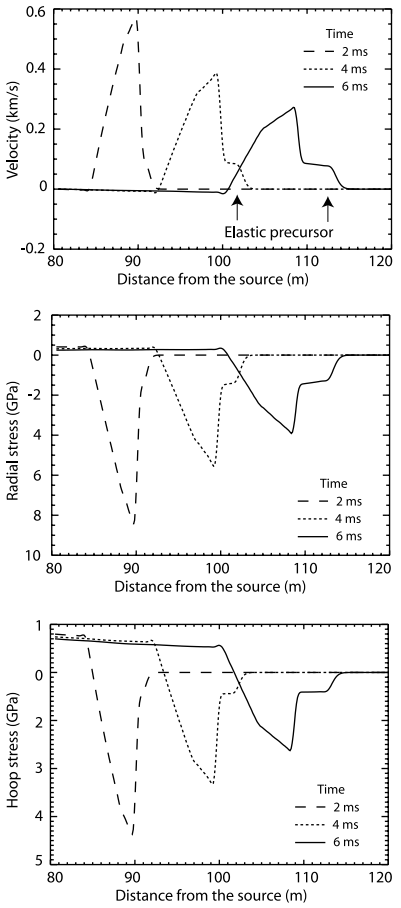

Fig. 1. The propagation of a compressive shock wave in spherical geometry derived from our numerical simulations. From top to bottom: velocity of the particle versus distance from the source, radial stress versus distance, and hoop stress versus distance (compression is negative). The elastic precursor is indicated by two arrows on the velocity graph. The hoop stress becomes tensional behind the shock. We suggest that this is the appropriate stress condition for the damage accumulation that leads to the formation of shatter cones.

spherical geometry using the numerical code SPALL [12]. SPALL is a one-dimensional Lagrangian hydrocode [13] that includes the Grady–Kipp–Melosh fragmentation model and uses a non-linear Murnhagan equation of state [14] and an elastic-plastic yield model [15]. We compute the propagation of a radially compressive stress wave with an initially triangular profile through a grid made of 300 cells. The rise time of the pulse is 0.1 ms and the decay time is 1 ms. The properties of the material are given in Tables 1 and 2. Many different computations with different initial shock waves were performed. All showed qualitatively similar behavior. We report here the detailed results of a computation of the propagation of a plastic wave in a spherical shell whose radius ranges between 80 and 120 m (see Fig. 1).

Both hoop and radial stresses are compressive during the rising portion of the wave and at some distance behind the shock front. An elastic precursor appears when the velocity of the plastic wave becomes slower than the velocity of sound. This situation occurs when the value of the pressure peak is just above the Hugoniot elastic limit (1 GPa in this computation). Actually, the parameters of simulations were chosen in order to observe a well developed elastic precursor. Indeed, the conditions required to observe this precursor are limited: the decrease of the stress in the spherical geometry implies that stresses close to the Hugoniot limit occur in a restricted region. During the decay of the plastic wave (never in the rising portion), the hoop stress becomes tensional while the radial stress is still compressive. The radial stress becomes slightly tensional at later time, but hoop stress is always the most tensional. This numerical simulation supports the existence of a tensional hoop stress occurring during the decay of the shock wave. We suggest that this hoop stress sets the stage for the tensional formation of shatter cones.

2.2. Description of the model

The mechanism we present here relies on the scattering produced by heterogeneities in the rocks. A tensional stress is required for the formation of shatter cones in our model. Our model relies on the interaction of a scattered elastic wave with the tensional hoop stress that develops behind the front in spherical geometry (Fig. 2). When the shock front encounters a heterogeneity whose material properties imply a lower sound speed (lower bulk modulus or higher density), an extensional wave is generated and propagates radially from the heterogeneity. In the case of high velocity heterogeneity, the scattered wave is compressive, and thus cannot lead to further ten-

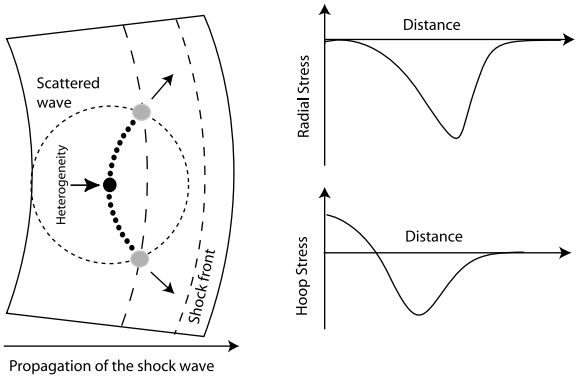

Fig. 2. Schematic representation of our model for the formation of shatter cones. Tensile fracture occurs at the intersection between the scattered tensile wave and the tensile hoop stresses in the main shock wave. When a critical value for the tensional stress is reached, the rock fractures in tension. The fractures accumulate on the surface of a conical region (indicated in the figure by filled circles and arrows).

sile fracture. As the main shock front propagates away from the site of the heterogeneity, the hoop stress, initially compressive reduces to zero and finally becomes tensional. Consider the total stress at any given time. The tensional hoop stress interferes constructively with the tensional scattered wave. For some critical value of the hoop stress, the interference produces a tensional stress above the tensile resistance of the material. Thus, fractures must occur first at the locations indicated by filled circles in Fig. 2.

The advance of both the scattered and the main shock waves produces fractures along a conical surface (actually, the exact shape of the structure is given by the successive intersections of two expanding spheres. This can be approximated by a cone for only a restricted range of distances). Fractures can potentially appear wherever the stress is above the tensile resistance of the material. However, the volume inside the conical surface is mechanically isolated from the surrounding rock mass and is thus preserved from further fracturing. The excess of tensional stress along the boundary of the cone localizes the fragmentation to a narrow region. One can argue that this tensional stress along the boundary of a cone is the precondition for the formation of striations according to the mechanism proposed by Sagy et al. [7].

Table 2
Material parameters

	Material	Heterogeneity
Density (kg/m^3)	3000	3000
Bulk modulus (GPa)	50	5
Shear modulus (GPa)	30	3
Murnhagan exponent	4	4
Hugoniot elastic limit (GPa)	50	50

3. Two-dimensional numerical model

3.1. Mesh geometry

The Navier–Stokes equations are solved in spherical geometry using the two-dimensional hydrocode SALE 2D. SALE 2D is capable of solving a wide range of problems, from low-velocity fluid flow to hypervelocity shock phenomena [16].

The Lagrangian mesh used in all simulations has the shape of a spherical shell defined by four parameters: the internal radius, the external radius, the angle and the radial dimension of the cells (see Fig. 3). To simulate a continuative boundary for the external surface and avoid any reflection of the direct wave from this boundary, the size of the last 20 cells is progressively increased by a factor of 1.1 for each successive layer.

3.2. The Grady–Kipp–Melosh fragmentation model

When stress becomes tensional our model employs the Grady–Kipp–Melosh dynamic fragmentation model [17,18] implemented in our version of SALE 2D. The effect of each individual fracture is integrated into a scalar parameter called damage, D, which is responsible for a linear decrease of the elastic moduli when the material is in tension. Damage is computed at each time step and can evolve for each cell from 0 (no failure) to 1 (cell is completely damaged and elastic moduli in tension have been decreased to 0). The reader is referred to the complete description of the numerical implementation of this model in [18].

3.3. Numerical stability

A shock wave is usually treated as a discontinuity in state variables [13] and must satisfy the Rankine–Hugoniot jump conditions. However, the numerical treatment of shock waves requires additional forces for the purpose of computational stability. Stability cannot be ensured by usual methods when such a discontinuity is present [19].

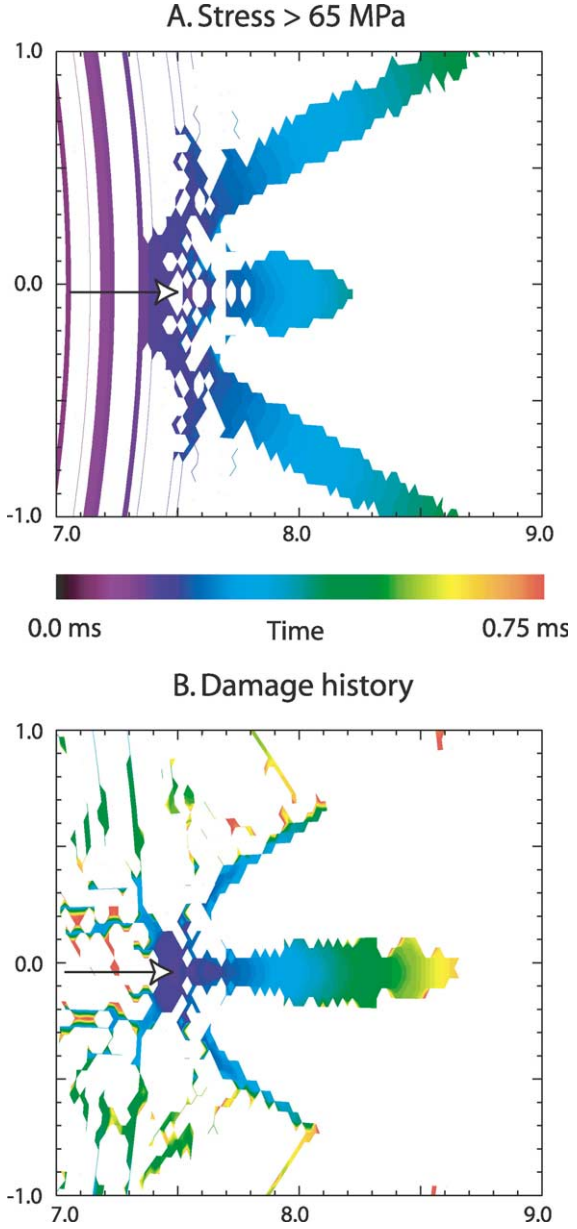

SALE 2D is capable of solving a wide range of problems, from low-velocity fluid flow to hypervelocity shock phenomena, with the help of artificial viscosity and coupling between adjacent nodes [16]. We use a value for the coefficient ARTVIS equal to 1.0 within SALE 2D for modeling the propagation of stress waves, since this was the lowest value that consistently maintains wave stability behind the front shock.

The effects of the artificial viscosity are negligible when shocks are not present. We have checked that the artificial viscosity does not affect the velocity and stress across the smeared-out jump, which accordingly obey the Hugoniot equations. To ensure numerical stability it has also been found necessary to use a physical viscosity. The use of a physical viscosity is supported by the explosion experiments in rock, reported in [20]. Values of 10 MPa-s are used in our simulations, as suggested by this study. This parameter does not affect the Rankine–Hugoniot conditions, but does have some effect on the rise time of the shock wave.

The fragmentation model implies an additional cost of computation, because damage accumulation in a failing cell is the fastest physical process. The time step is chosen to limit the damage increase in each cell to 3% per iteration as in [18].

4. Results

4.1. Conditions for the formation of shatter cones

Although the modification of the stress pattern

←

Fig. 3. (A) Stress history. Time at which the tensional stress exceeds the (average) minimum stress required for damage accumulation (see [18]). This plot illustrates how the stress responsible for the fragmentation propagates along the boundary of a cone as described in the text. (B) Time at which complete damage occurs. The duration of the computation is 0.75 ms. Damage accumulates when the tensional stress is greater than the minimum stress. The relief of the hoop stress as cells are fragmented limits further damage accumulation inside the cone (white cells have damage equal to 0). The two plots are not exactly identical since the maximum stress, which depends on the size of cells, varies along the radius of the spherical shell.

by the presence of a heterogeneity (described in Fig. 2) is qualitatively relevant to the formation of shatter cones, numerical simulations are required to investigate the exact conditions for such fractures. Indeed, once damage has accumulated for one cell, tensional stress is no longer transmitted by this cell, leading to a highly non-linear process. Thus, we investigate here the conditions suitable for shatter cones to form. The relevant parameters that might affect the formation of shatter cones include material properties (density, bulk and shear moduli, Hugoniot elastic limit) as well as the shape and magnitude of the stress wave.

In the simulations reported in this section, the angle of the spherical shell is 30° and the left boundary of the heterogeneity (toward the center of the spherical shell) is located at the 30th cell, corresponding to a distance of 7.60 m to the center of the spherical shell whose internal radius is 7 m. For example, when a region of two cells × two cells defines the area where a heterogeneity occurs, the corresponding dimensions are 4×7.2 cm. The size can be argued to be large compared with typical rock heterogeneities; however, we were limited by the computation time and thus the size of the elements of the mesh. The smallest heterogeneity in our simulations is composed of one cell.

The pulse has a triangular shape in all simulations and is defined by its maximum pressure, its rise time and the decay time factor (β), which is the ratio of the decay time to the rise time. The Hugoniot elastic limit is held at 50 GPa for these simulations, so that no plastic deformation occurs. The influence of plastic yielding will be addressed later.

4.2. Sound velocity of materials

We first investigated the properties required for a heterogeneity that produces a scattered wave strong enough to allow damage accumulation. The maximum pressure in the input pulse is 3 GPa, the rise time is 0.01 ms and the decay time factor 0.05. We will discuss later the relevance of these parameters to the real world. The simulations were performed with a constant density and four different bulk modulus ratios between the surrounding rock and the heterogeneity: 100, 10, 5 and 2 (the shear modulus is modified to hold the Poisson ratio constant). Since the sound velocity scales as the square root of these moduli, the velocity ratio ranges from 10 to $\sqrt{2}$. All other parameters are held constant. The stress and damage history (see Fig. 4, for a velocity ratio equal to $\sqrt{10}$) demonstrates that the model we propose can operate with these initial conditions. A cone is formed at the end of the simulation whose size is about 1 m at its base, and its apical angle is close to 90°.

From these simulations, it appears that a shatter cone develops for a velocity ratio greater than or equal to 2.2 (Table 3). Other simulations are required with different values of both density and bulk modulus to define more precisely those physical properties of the material and the heterogeneity that allow our mechanism to work. However, such velocity ratios are commonly seen in geological media as seen in [21] who reports data in the range of 1.5–7.8 km/s. Our mechanism is thus likely to occur in many different geological media.

4.3. Influence of the peak pressure

Next, we investigate the influence of the maximum pressure, as many authors report that shatter cones are only observed for a restricted range of pressures. The pulse shape is identical to the previous computation and the bulk modulus ratio is set to 10 (bulk modulus is 50 GPa and shear modulus is 30 GPa in the surrounding rock) which corresponds to a velocity ratio common

Table 3
Influence of the bulk modulus and the velocity ratio between the material and the heterogeneity

Bulk modulus of heterogeneity (GPa)	0.5	5.0	10.0	25.0
Bulk modulus ratio	100	10	5	2
Velocity ratio	10	3.2	2.2	1.4
Shatter cone	Yes	Yes	Yes	No

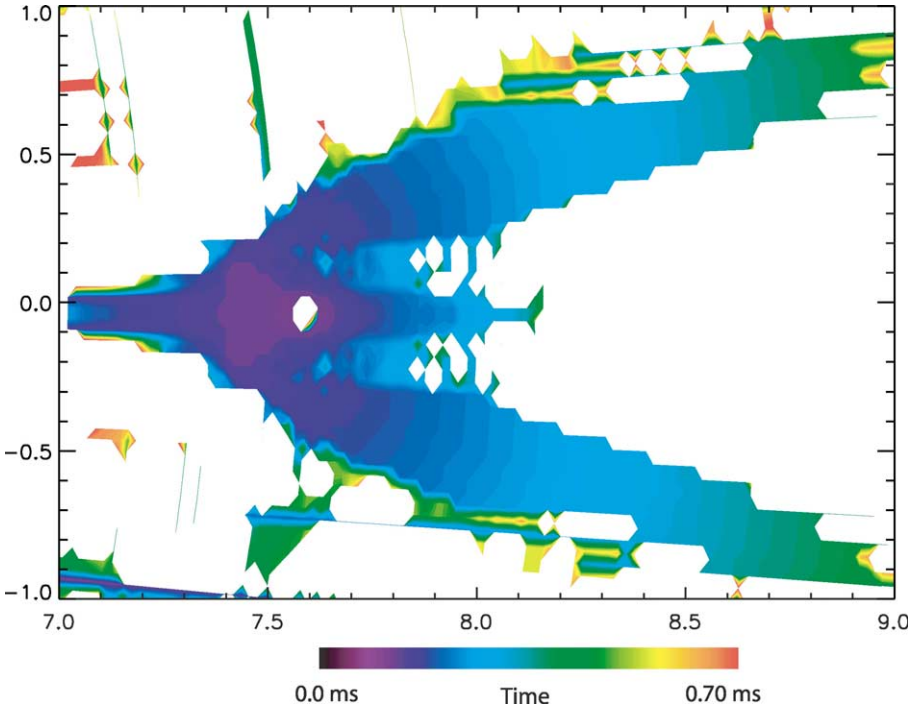

Fig. 4. Damage history. The duration of the computation is 0.70 ms. The fragmented region expands for the cells along the boundary of the cone, and the hoop stress is consequently relieved after damage occurs. The cells inside the cone remain intact (white cells are not damaged at any time) or only partially damaged.

in geological media. All parameters except pressure peak are held constant. The pressure peak is given as the input value of the pressure at the left boundary. The small decrease in pressure through our grid due to wave divergence in the spherical geometry is neglected when reporting the pressure conditions.

At pressures below 2 GPa, damage accumulates only in a restricted area at the edge of the heterogeneity and does not extend to other parts of the material. From 3 GPa to 6 GPa, a shatter cone develops. However, for the highest pressure, partial damage begins to accumulate even inside the cones. The region close to the heterogeneity is generally the most damaged region. This observation could explain the fact that shatter cones are commonly topless. At pressures above 7 GPa, damage is equal to 1 almost everywhere at the end of the computation. We interpret the upper limit for the pressure as follows: the ratio between the magnitude of the tensional stress resulting from the constructive interference and the hoop stress that occurs everywhere in the grid decreases at higher pressure. Consequently, the tensional hoop is not relieved fast enough along the boundary of the cone and thus accumulates more uni-

Table 4
Influence of the rise time and the size of the heterogeneity

Size of the heterogeneity (m)	0.04	0.04	0.04	0.08	0.08	0.08	0.16	0.16	0.16	0.4	0.4	0.4	0.8	0.8	0.8	1.6	1.6	1.6
Rise time of the stress wave (ms)	0.01	0.02	0.04	0.01	0.02	0.04	0.01	0.02	0.04	0.01	0.02	0.04	0.01	0.02	0.04	0.01	0.02	0.04
β (decay time factor)	5	5	5	5	5	5	5	5	5	5	5	5	5	5	5	5	5	5
Time ratio[a]	1.37	2.73	5.47	0.68	1.37	2.73	0.34	0.68	1.37	1.37	2.73	5.47	0.68	1.37	2.73	0.34	0.68	1.37
Shatter cone	Yes	Yes	No	Yes	Yes	No	Yes	Yes	Yes	Yes	Yes	No	Yes	Yes	No	Yes	Yes	Yes

[a] Time ratio is the rise in time to the time necessary for the wave to travel through the heterogeneity.

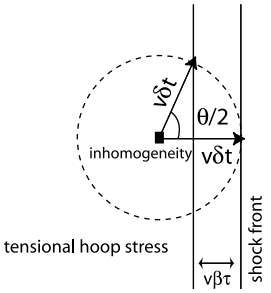

Fig. 5. Simple geometric model for the estimation of the apical angle of the shatter cone.

formly in the grid. The rock is crushed everywhere, but tensile failure does not concentrate along the surface of a cone. This model implies a continuous transition between shatter cone fractures and total fragmentation toward higher stresses.

The range of pressures suitable for the formation of shatter cones resulting from these simulations is in general agreement with the range of pressures observed in natural shatter cones or shatter cones formed in explosive experiments. The range of pressures observed for shatter cones therefore seems to be controlled by the dynamic resistance of the material in tension, and not by the Hugoniot limit as previously thought.

4.4. Influence of the rise time

Finally, we investigated the influence of the rise time of the pulse compared to the size of the heterogeneity, or the corresponding time for the wave to travel across the heterogeneity. We report the size of the heterogeneity along the radial direction, or along the propagation direction of the stress wave (see Table 4). Larger cells (20 cm instead of 2 cm) were used for the second set of the simulations, and the radius of the shell was also multiplied by a factor 10.

The occurrence of shatter cones seems to be highly correlated with the ratio between the rise time and the size of the heterogeneity. However, the rise time of a shock wave produced by high-velocity impact in geological media is unknown, since it has been never measured. It has often been assumed that the rise time is of the order of L/v where L is an equivalent radius of the projectile and v its velocity [14]. Adopting a reasonable ratio between the velocity of the projectile and the sound velocity in the target, the width of the pulse is a fraction of the size of the projectile. However, applying such a rationale, to most impact structures where shatter cones are observed, does not yield results consistent with the idea that shatter cones are produced by a centimeter- or millimeter-scale heterogeneity in the rock. Furthermore, our simulations demonstrate that shatter cones occur only when the ratio between the pulse width and the size of the heterogeneity is close to 1. To date, no good theoretical treatment of the shape of the shock wave is available. However, some experimental data have been acquired for shock waves from explosions [20] and laboratory impacts on metal targets [22]. These observations demonstrate, first, that the rise time and the shape of the shock are characteristics of the material and not of the source of the wave. Second, few relationships have been established experimentally between the rise time and the particle velocity. Consider, for example, the relationship derived from one of these experiments [20] for salt material:

$$\tau = 0.038 v_{\max}^{-0.6} \tag{1}$$

where τ is the rise time and $v_{\max}$ the maximum velocity of the particle. Using the Hugoniot equation and the material parameters used in our simulation, we derive:

$$\tau = 0.038 \left(\frac{P}{\rho U}\right)^{-0.6} = 900 P^{-0.6} \tag{2}$$

This experimental relationship has been validated for low-pressure shocks (in the range of 10–100 MPa). If we extrapolate this relation to a shock pressure of 3 GPa, we find a rise time of 1 ms still larger (by a factor 100) than the rise times we used in our computations. However, the non-linear increase of the velocity for high pressure may produce a thinner shock for stress waves of several GPa than that estimated by Eq. 2 above. Moreover, the presence of shatter cones at the scale of centimeters may indicate that the rise time of a stress wave produced by an impact is smaller than previously thought. On the other hand, if the widths of shock waves are as large

as a few meters in geological media, the hypothesis of an interaction between a direct wave and a scattered wave cannot be valid. The rise time of strong shock waves in geological media is an important, but presently unclear issue in our understanding of impact processes.

4.5. Example of formation of a shatter cone in a basaltic target

We present an example of a numerical simulation of the formation of a shatter cone (see Fig. 4), based on the hypothesis that an inclusion of ice is present in a basaltic material. Since we have explored the various ranges of conditions suitable for the formation of shatter cones with fictitious materials, we demonstrate here that the mechanism also operates in this particular and natural example. We used a mesh of 150×100 cells with an internal radius of 7 m. The radial size of the cells is 0.02 m. The angle of the spherical shell is 30°. The parameters of the two materials are given in Table 5. The Hugoniot limits of basalt and ice are poorly known, and we use very approximate values of respectively 1 and 0.1 GPa according to common ranges of values reported for a number of rocks [14]. The maximum of of the stress wave is 3 GPa, its rise time is 0.01 ms and its decay time is 0.05 ms.

5. Discussion and consequences for the analysis of shatter cone data

5.1. Comparison with other models

Different mechanisms have been proposed to explain the formation of shock-induced conical fractures. The most widely accepted mechanism was based on a theoretical study of the phenomenon by Johnson and Talbot [11]. They proposed that shatter cones form when the elastic precursor of the shock front is scattered by heterogeneity in the rock. The scattered elastic wave then interferes with the direct wave inside a conical region. Upon certain conditions, the plastic limit inside this conical region is exceeded, while stresses remain below this limit outside the volume. Then, Johnson and Talbot assumed that the stress is removed before the arrival of the plastic wave. Consequently, the material outside (which returns elastically to its original state) separates along the boundary of the cone which has been deformed plastically. However, both gage records from underground nuclear tests [23] and numerical simulations [24] (see also Fig. 1) show there is never a zero stress interval between the elastic precursor and the main plastic wave. Material could also relax behind an elastic wave, but it is not clear that such a relaxation produces suitable conditions for the operation of the Johnson–Talbot mechanism. Following these comments, Milton was the first to propose that shatter cones may form during the relaxation after the compression peak rather than before [6]. Recently, Sagy et al. proposed a model to explain the formation of striations and the geometry of a planar or slightly curved surface of fractures [7]. While this model is valuable for the interpretation of the branching microstructures commonly seen on the surfaces of shatter cones, it does not provide an explanation for the conical shape. The model we proposed appears to be the only one to explain the conical shape of these objects.

5.2. Required properties of the rock heterogeneities

Our proposed mechanism for the formation of shatter cones only operates if the impacted rock has heterogeneities with the following properties:

Table 5
Parameters of the embedding material and of the heterogeneity (ice) [20,22]

	Density (kg/m^3)	Bulk modulus (GPa)	Shear modulus (GPa)	Murnhagan exponent	c_g (m/s)	pweib (m)	cweib (m^{-3})
Embedding material	2980	60.1	36.7	5.5	1790	9.05	3.05×10^{40}
Heterogeneity	900	0.2	0.12	5.23	7500	8.7	3.2×10^{44}

(1) the shock wave must travel faster in the rock than in the heterogeneity by a minimum factor of about 2, (2) the dimensions of the heterogeneity must be comparable to the width of the shock wave which are both smaller than the related shatter cone. The first property is not rare in geological media. Smaller heterogeneities like vesicles in basalt may be more common than the one used in our last natural simulation. However, we do not have very strong constraints on the pulse width since it was measured in only one experiment and extrapolated here to a higher pressure level. Depending of the pulse width, heterogeneities at all scales can potentially form shatter cones and the large size of heterogeneities used in our natural simulation must not be seen as a necessary condition for the model to operate in natural conditions.

5.3. Consequences

Apical angles of shatter cones vary from 60 to 120°. These simulations do not yet fully define all of the parameters that influence the apical angle of the cones. One of the main factors must be the decay time, which has a direct influence on the delay between the passage of the shock front and the arrival of the tensional hoop stress.

A simple geometric model highlights the factors relevant to the determination of the apical angles in shatter cones. Consider, as a first order approximation, that the delay between the shock wave and the tensional hoop stress is equal to the decay time of the stress wave $\beta\tau$, where τ is the rise time. If the radius of the direct shock wave is large, the front can be approximated by a plane, at least for small distances compared to the radius, and the angle of the shatter cone is (see Fig. 5):

$$\theta(t) = 2\arccos\left(1-\frac{\beta\tau}{\delta t}\right) \quad (3)$$

where δt is the time elapsed since the contact between the shock front and the heterogeneity. The reported angles of shatter cones (60–120°) correspond to values of $\delta t/\tau$ that range from 2 to $2/\sqrt{3}$. The damage begins to accumulate at the location of the interference. Since fracturing is a very fast process, we checked that Eq. 3 applies to the shape of the fracture when t is approximated by the time when the damage of a cell is equal to 1.

In conclusion, this formula indicates, first, that the apparent apical angle observed on a part of a shatter cone depends on the decay time of the shock wave. Second, this approximate formula also illustrates the influence of the parameters of the heterogeneity: the magnitude of the extensional and spherical scattered wave decreases during its propagation and the maximum time δt during which this wave is strong enough to initiate damage only along the boundary of the conical region depends on the properties of the heterogeneity, in particular the sound velocity ratio between the heterogeneity and the surrounding material. The influence of all these factors must be explored further by means of numerical simulations to interpret the apical angle data of shatter cones and their likely variations as a function of distance to the source.

5.4. Suggestions of specific tests to validate the model

The validation of the model by new field measurements is beyond the scope of this paper. However, it is suggested here to measure shapes, sizes and distribution of shatter cones in various impact sites. Measurements of apical angle directly on a complete cone are very rare and are usually obtained by synthetic stereoplots of many cones in a given exposure. Actually, the knowledge of the global shape of the surface fracture would be more relevant than the apical angle to validate our model and requires new observations. Rocks contain plenty of heterogeneity at all scales. From our model, the nature and sizes of heterogeneity are strongly correlated with the distribution and sizes of shatter cones. Another aspect of the validation of the model by field measurements would be a detailed characterization of the nature at different scales of rock heterogeneities where shatter cones are observed.

6. Conclusion

A new model for the formation of shatter cones

has been investigated by means of numerical simulations. The mechanism proposed here operates over a wide range of conditions and for materials with properties similar to common geological media. However, the mechanism operates only within a restricted range of pressures, 3–6 GPa, which is close to the range of pressures derived from observations of both natural shatter cones and shatter cones produced by explosion experiments. The model gives results consistent with the reported apical angles and the observation that cones commonly point toward the source (deviations from this relationship may be due to scattering and consequent non-radial propagation of the main shock wave). Following the results of the numerical simulations, the size and distribution of shatter cones in impact structures must be correlated with the ratio between the size of the heterogeneity and the pulse width of the shock wave. This prediction implies that the rise time of shock wave in geological media is shorter than previously believed, otherwise this mechanism cannot operate. This fundamental issue may be investigated through the analysis of shapes, sizes and distribution of shatter cones on various impact sites and the analysis of rock heterogeneities. According to this model, the apical angle depends on both the properties of the heterogeneity and the decay time of the shock wave. None of these simulations, except the inclusion of ice in basalt, includes a significant amount of plastic deformation. The Hugoniot elastic limits of rocks vary considerably even among rocks of the same type, and thus the effect of plastic deformation during the fragmentation invites further study.

Acknowledgements

This work was performed during a visit of D.B. to the Lunar and Planetary Laboratory, University of Arizona. It was supported by NASA Grant NAG5-11493 and a post-doctoral fellowship from CNES. Thoughtful reviews by Ze'ev Reches and Amos Nur provided many well appreciated suggestions and constructive criticisms.*[VC]*

References

[1] R.S. Dietz, Meteorite impact suggested by shatter cones in rock, Science 131 (1960) 1781–1784.
[2] D.J. Roddy, L.K. Davis, Shatter cones formed in large-scale experimental explosion craters, in: D.J. Roddy, R.O. Pepin, R.B. Merill (Eds.), Impact and Explosion Cratering, Pergamon Press, New York, 1977, pp. 715–750.
[3] B.M. French, Traces of Catastrophe: A Handbook of Shock-Metamorphic Effects in Terrestrial Meteorite Impact Structures, LPI Contribution No. 954, Lunar and Planetary Institute, Houston TX, 1998, 120 pp.
[4] E. Schneider, G.A. Wagner, Shatter cones produced experimentally by impacts in limestone targets, Earth Planet. Sci. Lett. 203 (1976) 40–44.
[5] L.O. Nicolaysen, W.U. Reimold, Vredefort shatter cones revisited, J. Geophys. Res. 104 (1999) 4911–4930.
[6] D.J. Milton, Shatter cones – An outstanding problem in shock mechanics, in: D.J. Roddy, R.O. Pepin, R.B. Merill (Eds.), Impact and Explosion Cratering, Pergamon Press, New York, 1977, pp. 703–714.
[7] A. Sagy, Z. Reches, J. Finegerg, Shatter-cones: Dynamic fractures generated by meteoritic impacts, Nature 418 (2002) 310–313.
[8] R.M. Stesky, H.C. Halls, Structural analysis of shatter cones from the state Islands, northern Lake Superior, Can. J. Earth Sci. 20 (1983) 1–18.
[9] N.L. Gay, Spherules on shatter cones surfaces from the Vredefort structure, South Africa, Science 194 (1972) 724.
[10] H.M. Gibson, Shock-induced melting and vaporization of shatter cones surfaces: Evidence from the Sudbury impact structure, Meteorit. Planet. Sci. 33 (1998) 329–336.
[11] G. Johnson, R. Talbot, A Theoretical Study of the Shock Wave Origin of Shatter Cones, M.S. Thesis, Air Force Int. Tech, Wright-Patterson AFB, OH, 1969, 170 pp.
[12] H.J. Melosh, High-velocity solid ejecta fragments from hypervelocity impacts, Int. J. Impact Eng. 5 (1987) 483–492.
[13] R.D. Richtmyer, K.W. Morton, Difference Methods for Initial-Value Problems, Interscience, New York, 1967.
[14] H.J. Melosh, Impact Cratering, A Geologic Process, Oxford University Press, New York, 1989, 245 pp.
[15] C.E. Anderson, An overview of the theory of hydrocodes, Int. J. Impact Eng. 5 (1987) 33–59.
[16] A. Amsden, H.M. Ruppel, C.W. Hirt, SALE: A Simplified ALE Computer Program for Fluid Flow at All Speeds, LA-8095, Los Alamos National Laboratory, Los Alamos, CA, 1980.
[17] D.E. Grady, M.E. Kipp, Continuum modeling of explosive failure in oil shale, Int. J. R. Mech. Min. Sci. Geomech. Abstr. 17 (1980) 147–157.
[18] H.J. Melosh, E.V. Ryan, Dynamic fragmentation in impacts: Hydrocode simulation of laboratory impact, J. Geophys. Res. 97 (1992) 14735–14759.
[19] J. Von Neumann, R.D. Richtmyer, A method for the numerical calculation of hydrodynamic shocks, J. Appl. Phys. 21 (1950) 232–237.

[20] H.J. Melosh, Shock viscosity of explosion waves in geologic media, J. Appl. Phys. (submitted).
[21] F. Birch, Compressibility; Elastic constants, in: S.P. Clark (Ed.), Handbook of Physical Constants, GSA Memoir 97, Geological Society of America, New York, 1966, pp. 107–173.
[22] J.W. Swegle, D.E. Grady, Shock viscosity and the prediction of shock wave arrival times, J. Appl. Phys. 58 (1985) 603–701.
[23] W.R. Perret, R.C. Bass, Free-Field Ground Motion Induced by Underground Explosions, SAND74-0252, Sandia National Lab, 1975.
[24] D.E. Grady, Processes occurring in shock wave compression of rocks and minerals, in: M.H. Manghanani, S.-I. Akimoto (Eds.), High-Pressure Research: Applications in Geophysics, Academic Press, New York, 1977, pp. 389–438.